Missouri University of Science and Technology

Scholars' Mine

Civil, Architectural and Environmental Engineering Faculty Research & Creative Works

Civil, Architectural and Environmental Engineering

01 Oct 2022

Homogenous Flow Performance of Steel Fiber-Reinforced Self-Consolidating Concrete for Repair Applications: Developing a New Empirical Set-Up

Naimeh Nouri

Masoud Hosseinpoor

Ammar Yahia

Kamal Khayat
Missouri University of Science and Technology, khayatk@mst.edu

Follow this and additional works at: https://scholarsmine.mst.edu/civarc_enveng_facwork

 Part of the Architectural Engineering Commons, and the Civil and Environmental Engineering Commons

Recommended Citation

N. Nouri et al., "Homogenous Flow Performance of Steel Fiber-Reinforced Self-Consolidating Concrete for Repair Applications: Developing a New Empirical Set-Up," *Materials and Structures/Materiaux et Constructions*, vol. 55, no. 8, article no. 223, Springer, Oct 2022.
The definitive version is available at https://doi.org/10.1617/s11527-022-02056-x

This Article - Journal is brought to you for free and open access by Scholars' Mine. It has been accepted for inclusion in Civil, Architectural and Environmental Engineering Faculty Research & Creative Works by an authorized administrator of Scholars' Mine. This work is protected by U. S. Copyright Law. Unauthorized use including reproduction for redistribution requires the permission of the copyright holder. For more information, please contact scholarsmine@mst.edu.

Materials and Structures (2022) 55:223
https://doi.org/10.1617/s11527-022-02056-x

ORIGINAL ARTICLE

Homogenous flow performance of steel fiber-reinforced self-consolidating concrete for repair applications: developing a new empirical set-up

Naimeh Nouri · Masoud Hosseinpoor · Ammar Yahia · Kamal H. Khayat

Received: 18 June 2022 / Accepted: 27 September 2022 / Published online: 14 October 2022
© The Author(s) 2022

Abstract In this study, a new empirical Square-Box test was employed to evaluate the homogeneous flow performance of fiber-reinforced self-consolidating concrete (FR-SCC) under confined-flow conditions that are typical of repair applications. The Square-Box set-up consisted of a closed-circuit box, providing 2.4-m flow distance and a closed-surface cross section of 100-mm width and 200-mm height, equipped with 0 and 4 rows of reinforcing bar grids with 45-mm clear spacing. The flow performance was assessed in terms of dynamic stability and passing ability. The investigated mixtures were considered as diphasic suspensions of fiber-coarse aggregate (F-A > 5 mm) in suspending mortars containing particles finer than 5 mm. According to the experimental results, the dynamic segregation and blocking indices of the investigated mixtures were found in good agreements with characteristics of F-A combination and rheology of mortar. The investigated mixtures exhibited significantly higher blocking indices through the Square-Box set-up compared to those obtained using the L-Box test. Furthermore, the characteristics of F-A and rheology of mortar showed opposite effects on dynamic segregation assessed using Square-Box and conventional T-Box set-ups. Under confined flow conditions, higher dynamic segregation led to more dissimilar compressive strength values at different flow distances through the proposed Square-Box set-up. A new filling ability classification was established based on the experimental dynamic stability and passing ability results of the proposed empirical test.

Keywords Blocking · Dynamic segregation · Fiber-reinforced self-consolidating concrete · Repair · Rheology · Square-Box test

N. Nouri · M. Hosseinpoor (✉) · A. Yahia
Department of Civil and Building Engineering, Université de Sherbrooke, Sherbrooke, QC, Canada
e-mail: Masoud.Hosseinpoor@Usherbrooke.ca

K. H. Khayat
Department of Civil, Architectural and Environmental Engineering, Center for Infrastructure Engineering Studies, Missouri University of Science and Technology, Rolla, MO, USA

1 Introduction

Self-consolidating concrete (SCC) has gained high interest in construction industry given its ability to facilitate the casting of highly congested elements and filling narrow gaps in formwork systems. However, cementitious materials are generally considered as brittle, with low tensile and flexural strengths and weak strain capacity [1]. Concrete is thus reinforced by reinforcement bars [2] and steel fibers [3] to improve strength-strain capacity and ductility of concrete structures. Conventional reinforcement bars

can be partially replaced by steel fibers while maintaining the required flexural and tensile strengths [4, 5]. Steel fibers can improve the crack resistance and energy absorption (toughness), as well as impact and fatigue resistance [6, 7]. Song et al. [8] reported an improvement of flexural strength of ultra-high-performance fiber-reinforced concrete by increasing the steel fiber content. Zhang et al. [9] reported that increasing the fiber content from 0.5 to 2% can enhance compressive, tensile, and flexural strengths of fiber-reinforced concrete (FRC) by 4–24%, 33–122%, and 25–111%, respectively.

Combining the advantages of SCC and FRC [4], fiber-reinforced self-consolidating concrete (FR-SCC) has gained acceptance in different applications, such as precast industry [5], rehabilitation of transportation infrastructure [3], construction of slabs on grade [10], slabs on piles [11], and tunneling applications [11]. However, adding fibers to SCC can significantly decrease its workability [12]. This can increase the risk of blockage of fibers and aggregate behind the reinforcing bars during casting [13]. An uneven fiber-aggregate distribution and fiber orientation can negatively affect the mechanical performance of FR-SCC [14]. The fiber distribution is a function of rheological properties of concrete, flow distance, and arrangement of reinforcing bars [4, 13, 15]. Jasiūnienė et al. [15] reported the most uneven fiber distribution through a beam for the FR-SCC mixtures with the lowest viscosity. Ferrara et al. [4] reported the negative effect of lowering the viscosity of FR-SCC on its static stability. Moreover, Jasiūnienė et al. [15] and Yoo et al. [16] reported a heterogeneous distribution of fibers at longer flow distances in the formwork. On the other hand, Žirgulis et al. [13] highlighted the effect of reinforcing bars configuration on fiber distribution. The authors reported the maximum fiber blockage within two layers of reinforcing bars compared to the configuration equipped with one layer of reinforcement.

FR-SCC is specified as a promising repair material to enhance the cracking resistance and service life of repair subjected to a high degree of restrained shrinkage [17–24]. Early application of FR-SCC involved the use of 0.25%, by volume, synthetic structural fibers for the rehabilitation of the Jarry/Querbes underpass in Montreal, Canada [22]. An extensive investigation to evaluate the workability, mechanical performance, shrinkage resistance, and durability of FR-SCC types targeted for repair applications was carried out by Hwang and Khayat [17] and Kassimi et al. [18, 23]. Hwang and Khayat [17] reported that the increase in synthetic fiber volume up to 0.5% led to an approximately 40% increase in the elapsed time before restrained shrinkage crack initiation. Kassimi et al. [18] showed that repair with FR-SCC mixtures containing up to 0.5% steel and multifilament polypropylene fibers can restore at least 95% of the initial load-carrying capacity of structural elements made of conventional-vibrated concrete. Kassimi et al. [23] reported lower crack width of composite beams repaired with FR-SCC due to enhanced fiber orientation along the tension zone and concrete confinement during casting.

FR-SCC can properly fill the narrow sections to be repaired and pass through the congested reinforcement bars under its own weight with low risk of blockage and instability which cannot be achieved using conventional or flowable concrete. Unlike free-surface flow in casting process of concrete, close-surface flows are encountered in repair applications, hence leading to extremely higher confinement. Indeed, the repair zones are typically located at the densely reinforced tension zones in concrete (RC) elements. For instance, Safdar et al. [19] repaired lower sections of 3-m long RC beams using FR-SCC mixtures that were horizontally cast through narrow repaired zones of 20–60 mm thicknesses in presence of 10- and 16-mm diameter rebars. Different FR-SCC types were used to repair various RC beams [18, 23]. The repair material was placed through vertical 140-mm diameter holes, passing across 10- and 20-mm diameter rebars to repair a 125-mm thickness zone at the bottom side of the 3.2-m long beams [18, 23]. Arezoumandi et al. [22] applied FR-SCC to repair 75-mm thickness of 510-mm long flexural prisms and 125–175 mm thickness of bottom zones of 4.3-m long RC beams that are reinforced with 19-mm rebars. In order to enhance the bond between the repair FR-SCC and substrate concrete, the surface of the existing concrete is usually roughened using hydro-demolition [18, 19, 23].

The additional confinement and friction exerted on repair FR-SCC can increase the interaction between the fibers and coarse aggregate with formwork walls and reinforcing bars, hence leading to high risks of granular blocking in highly confined regions. FR-SCC mixture design should be tailored by taking into

account geometric conditions, such as the clear spacing between the formwork and concrete substrate, density and spacing of the reinforcing bars. The type and volume of fibers, particle-size distribution of aggregate, as well as the workability and rheological properties of the paste/mortar matrix must be optimized. Understanding the coupled effect of the aforementioned parameters on homogenous performance of FR-SCC allows to secure proper mechanical performance of the cast element. Indeed, high flowability, dynamic stability, and passing ability of FR-SCC can ensure successful casting and targeted mechanical performance at different flow distances passing through the reinforced elements.

Voigt et al. [25] investigated the performance of FRC mixtures using a diphasic concept. The granular skeleton and fibers, as the solid phase, and the mortar matrix, as the liquid phase filling the interparticle voids and lubricating the solid dispersions, were investigated. Koura et al. [26] and Hosseinpoor et al. [27, 28] studied the workability of SCC as a biphasic suspension of coarse aggregate (> 1.25 mm) and fine mortar (< 1.25 mm). Koura et al. [26] investigated the coupled effect of coarse aggregate characteristics and fine mortar rheology on dynamic stability of SCC. The dynamic segregation of SCC was measured by variation of the relative-solid packing-fraction of coarse aggregate (φ/φ_{max}), defined by the ratio of their volumetric content (φ)-to-their packing density (φ_{max}), in the T-Box set-up [29]. The φ/φ_{max} of coarse aggregate showed a dominant effect on dynamic stability of SCC compared to the rheological properties of fine mortar [26]. Hosseinpoor et al. [28] evaluated the blocking resistance of SCC by variation of the φ/φ_{max} of coarse aggregate passing across the rebars in the J-Ring [30] and L-Box [31] set-ups. The authors reported the negative effect of decreasing rheological properties of fine mortar, as well as increasing φ/φ_{max} of coarse aggregates on passing ability of SCC. Moreover, the study revealed a decrease of risk of blocking by lowering the water-to-binder ratio (W/B), dosage of high-range water-reducer (HRWR), and the paste volume (V_P).

The flow performance of SCC and FR-SCC mixtures can be evaluated using different empirical tests, such as slump flow [32], J-Ring [30], U-Box [31, 33], L-Box [31], and filling-box [34] test set-ups. However, the short flow distance through slump flow, J-Ring, L-Box, U-Box, and filling-box tests is not representative to those traveled by concrete during real-scale castings. Accordingly, Jasiūnienė et al. [15] and Ferrara et al. [4] used beams of 1.35 ± 0.15 m length to evaluate the flow homogeneity and fiber orientation of FR-SCC mixtures. However, these beams were not equipped with reinforcement bars. The heterogeneity of concrete can be more critical in the presence of reinforcing bars and formwork walls (blocking and wall effect), which are more critical in confined repair sections. The arrangement, diameter, and spacing of reinforcing bars can significantly affect the passing ability of FR-SCC mixtures containing rigid fibers.

Conventional workability tests used for SCC and those developed for FRC cannot be properly applied to evaluate the flow performance of FR-SCC for repair applications. A new empirical method is required to simulate concrete flow in confined and restricted flow conditions, such as those encountered in repair applications. A new empirical Square-Box set-up was developed to evaluate the coupled effect of fiber volume, φ/φ_{max} of fiber-coarse aggregate combination, as well as the rheological properties of the suspending mortar on dynamic stability and passing ability of FR-SCC. The Square-Box test allows concrete to travel a horizontal distance of 2.4 m passing through a close-surface and close-circuit narrow channel (100-mm width) equipped with various congested reinforcing bars with clear spacing of 45 mm. FR-SCC mixtures exhibiting high passing ability and good dynamic stability determined using conventional L-Box and T-Box tests were selected. The study aimed at proposing a filling ability classification for FR-SCC that can secure adequate homogeneous flow performance in confined areas. The impact of heterogeneous flow on the uniformity of in-situ mechanical properties was also evaluated.

2 Experimental study

2.1 Proportioning of the investigated FR-SCC mixtures: materials and characterizations

A natural-river sand (0–5 mm) and two different classes of crushed-limestone coarse aggregate of 5–10 mm (CA1) and 5–14 mm (CA2) were used (Table 1). As shown in Table 1, three different combinations (PSD-1 to PSD-3) of coarse aggregate

Table 1 Particle-size distribution of the fine and coarse aggregates and their combinations (PSD-1-3) made with different volumetric proportions of CA1-3 coarse aggregate classes

Sieve size (mm)	Sand	CA1	CA2	PSD-1: 100% CA1	PSD-2: 80% CA1 + 20% CA2	PSD-3: 60% CA1 + 40% CA2
20	100	100	100	100	100	100
14	100	100	85.5	100	97.1	94.2
10	100	81.7	48.9	81.7	75.1	68.6
5	99.4	10.2	5.7	10.2	9.3	8.4
2.5	83.6	4.9	1.5	4.9	4.2	3.5
1.25	67.3	3.9	1.2	3.9	3.3	2.8
0.630	49.5	–	–	–	–	–
0.315	23.7	–	–	–	–	–
0.160	6.6	–	–	–	–	–
0.080	2.9	–	–	–	–	–
Specific gravity	2.67	2.72	2.73	–	–	–

were considered to achieve different levels of packing densities. The investigated FR-SCC mixtures were proportioned with a volumetric sand-to-total aggregate ratio of 0.55. Moreover, a hooked end steel fiber with 30-mm length, 0.55-mm diameter (aspect ratio of 55), and modulus of elasticity of 200 GPa was also used.

Various fiber volumes of 0.4–0.9% were mixed with the 3 coarse aggregate mixtures PSD1-3. The packing density of the investigated F-A mixtures were evaluated using the dry method and intensive compaction tester (ICT) [35–37]. Three F-A mixtures corresponding to the minimum, medium, and maximum packing density (PD) values of 0.536, 0.544, and 0.554 were selected to cover a wide range of packing density. Nine FR-SCC mixtures (FRC-1-9) were then proportioned with coarse aggregate combinations PSD1-3, W/B of 0.42, and V_P of 0.27, 0.30, and 0.33, as summarized in Table 2. Khayat et al. [3] recommended an upper limit of fiber volume of 0.5% of macro steel fibers (out of unit volume of concrete) to ensure proper workability for SCC. Accordingly, an additional F-A mixture was proportioned with PSD3 and 1.77% fiber volume. This F-A mixture corresponded to 0.5% fiber volume in 1 m^3 of concrete mixture (FRC-10) containing V_P of 0.33 (Table 2).

A ternary-blended cement made with 70% general use Portland cement (GU), 25% class F fly ash, and 5% silica fume was used. A polycarboxylate-based HRWR and an air-entraining agent (AEA) was used to achieve a targeted slump-flow value of 680 ± 20 mm and air content of 5–8%, respectively. All the mixtures were prepared in batches of 65 L using a rotating drum mixer. The 28-day compressive strength ($f'_{c\text{-}Ref}$) determined using cylindrical samples measuring 100-mm diameter and 200-mm height are presented in Table 2.

2.2 Conventional workability measurements

The blocking resistance and dynamic stability of the investigated mixtures were firstly evaluated using the L-Box and T-Box tests, respectively. The L-Box set-up has a vertical part measuring 600-mm, a horizontal channel of 700-mm length and 200 mm in width [3]. Two 10-mm diameter reinforcing bars are installed right after the separating gate. Two 100 × 200-mm cylindrical samples were taken from the fresh concrete at the two lateral sides of the L-Box set-up. The concentration and packing density of F-A portions in the samples taken behind the rebars and end of the horizontal channel of the L-Box set-up were determined. The ultimate blocking index in the L-Box test (UBI_{LB}) was evaluated, as follows:

$$UBI_{LB}\ (\%) = \frac{\left(\frac{\varphi}{\varphi_{max}}\right)_B - \left(\frac{\varphi}{\varphi_{max}}\right)_E}{\left(\frac{\varphi}{\varphi_{max}}\right)_{Ref}} \times 100\% \quad (1)$$

where $\left(\frac{\varphi}{\varphi_{max}}\right)_B$, $\left(\frac{\varphi}{\varphi_{max}}\right)_E$, and $\left(\frac{\varphi}{\varphi_{max}}\right)_{Ref}$ corresponds to

Table 2 Proportioning and workability results of the investigated FR-SCC mixtures (HRWR and AEA dosages are in ml/100 kg of binder)

Mix	Binder (kg/m^3)	V_P (%)	Sand (kg/m^3)	PSD of CA	CA1 (kg/m^3)	CA2 (kg/m^3)	Fiber (kg/m^3)	V_f in F-A mixture (%)	V_f in concrete (%)
FRC-1	352	27	999	PSD-1	825	0	22	0.9	0.28
FRC-2	352	27	999	PSD-2	661	166	17	0.7	0.22
FRC-3	352	27	999	PSD-3	497	333	9	0.4	0.12
FRC-4	392	30	955	PSD-1	789	0	20	0.9	0.26
FRC-5	392	30	955	PSD-2	632	159	16	0.7	0.20
FRC-6	392	30	955	PSD-3	475	318	9	0.4	0.12
FRC-7	431	33	910	PSD-1	752	0	20	0.9	0.25
FRC-8	431	33	910	PSD-2	603	151	15	0.7	0.20
FRC-9	431	33	910	PSD-3	454	303	9	0.4	0.11
FRC-10	431	33	910	PSD-3	447	299	39	1.77	0.50

Mix	φ_{max} of F-A mixture	φ/φ_{max} of F-A	HRWR	AEA	Air content (%)	Slump flow (mm)	$f'_{c\text{-}Ref}$ (MPa)*	UBI_{LB} (%)	$UDSI_{TB}$ (%)
FRC-1	0.536	0.571	3300	5	6.3	667	30.2	79.7	0.4
FRC-2	0.544	0.563	2860	5	6.1	665	31.6	47.3	17.7
FRC-3	0.554	0.552	2600	5	7.6	662	33.2	12.0	12.2
FRC-4	0.536	0.546	1500	5	7.4	700	38.9	19.5	20.4
FRC-5	0.544	0.538	1350	10	6.7	673	39.9	14.3	18.4
FRC-6	0.554	0.528	1180	8	7.2	656	47.8	18.1	40.3
FRC-7	0.536	0.521	1140	9	7.8	678	42.9	14.6	49.6
FRC-8	0.544	0.513	980	7	7.9	685	44.7	16.7	71.4
FRC-9	0.554	0.503	820	7	7.5	694	46.0	9.8	54.8
FRC-10	0.534	0.523	1036	7	7.7	675	49.4	11.4	40.6

*Standard deviations of all the compressive strength measurements ranged between 0.1 and 1.3 MPa

the relative-solid packing fraction of F-A mixtures in samples taken from behind the rebars and end of horizontal channel of the L-Box set-up, as well as reference mixture, respectively. Moreover, the dynamic stability of the investigated FR-SCC mixtures was investigated using the T-Box set-up [29] (16-L sample) under 60 tilting cycles of 2-s period. Two cylindrical samples were taken from the tilt-up (TU) and tilt-down (TD) sections. The volumetric content and packing density of the F-A portion of the taken samples were determined. The ultimate dynamic segregation index ($UDSI_{TB}$) of the investigated mixtures in T-Box test was assessed, as follow:

$$UDSI_{TB}\ (\%) = \frac{\left(\frac{\varphi}{\varphi_{max}}\right)_{TD} - \left(\frac{\varphi}{\varphi_{max}}\right)_{TU}}{\left(\frac{\varphi}{\varphi_{max}}\right)_{Ref}} \times 100\% \qquad (2)$$

where $\left(\frac{\varphi}{\varphi_{max}}\right)_{TD}$, $\left(\frac{\varphi}{\varphi_{max}}\right)_{TU}$, and $\left(\frac{\varphi}{\varphi_{max}}\right)_{Ref}$ are the volumetric content-to-packing density ratios of the F-A mixtures corresponding to the samples taken from tilt-down and tilt-up zones of the T-Box set-up, and reference mixture, respectively. The results of the workability tests are summarized in Table 2. It is worth mentioning that due to the highly restricted flow conditions of repair application, a particular attention should be considered to ensure high passing ability of FR-SCC for repair application rather than their dynamic stability. Therefore, according to the workability results presented in Table 2, six mixtures exhibiting high passing ability and medium to high dynamic stability, corresponding to the UBI_{LB} values less than 27% and $UDSI_{TB}$ values less than 50%, respectively, were selected for further analyses.

2.3 Rheological evaluation of suspending paste/mortar

The rheological properties of the suspending mortar (< 5 mm) of the FR-SCC mixtures were assessed considering a diphasic approach proposed by Hosseinpoor et al. [38, 39]. The mortar matrix (< 5 mm) was considered as a diphasic suspension of coarser particles of sand (> 1.25 mm) and fine mortar (< 1.25 mm). Similarly, the fine mortar was investigated as a suspension of fine sand particles (< 1.25 mm) in a suspending cement paste. According to the diphasic models proposed by Hosseinpoor et al. [38, 39], the volumetric content and packing density of fine (FS < 1.25 mm) and coarse (1.25 mm < CS < 5 mm) particles of sand suspended in cement pastes and fine mortars, respectively, as well as the yield stress and plastic viscosity of cement paste ($\tau_{0\text{-}P}$, $\mu_{p\text{-}P}$) and fine mortar ($\tau_{0\text{-FM}}$, $\mu_{p\text{-FM}}$) mixtures were considered. The rheological properties ($\tau_{0\text{-FM}}$, $\mu_{p\text{-FM}}$) of fine mortar mixtures (< 1.25 mm) were evaluated as functions of the rheological properties of their corresponding cement pastes ($\tau_{0\text{-}P}$, $\mu_{p\text{-}P}$) and relative-solid packing fraction of fine sand ($\varphi_{FS}/\varphi_{max\text{-}FS}$) suspended in the cement pastes. Subsequently, the yield stress ($\tau_{0\text{-}M}$) and plastic viscosity ($\mu_{p\text{-}M}$) of the mortar matrices (< 5 mm) were evaluated as functions of yield stress ($\tau_{0\text{-FM}}$) and plastic viscosity ($\mu_{p\text{-FM}}$) of their corresponding fine mortars and relative-solid packing fraction of fine sand ($\varphi_{CS}/\varphi_{max\text{-}CS}$) suspended in the fine mortars. It is worth mentioning that the rheological properties of the cement paste mixtures were evaluated using a 50-mm diameter parallel-plates system and a 4-mm gap. The shear protocol included applying a pre-shearing of 150 s^{-1} for 120 s, then stepwise descending shear rate values from 150 to 1 s^{-1} during 150 s in 6 steps. The rheological properties of the investigated mortar mixtures and their corresponding cement paste mixtures are summarized in Table 3.

2.4 Workability measurements using new square-box set-up

A new Square-Box test set-up is proposed to investigate the homogeneous flow of FR-SCC under confined flow conditions. As shown in Fig. 1, the Square-Box set-up consists of a close-circuit of four close-surface rectangular channels measuring 200 mm in height, 700 mm in length, and 100 mm in width, yielding a box with 700 × 700 mm outer dimensions, 500 × 500 mm inner dimensions, and a height of 200 mm. A sample of 48 L of concrete was cast in a continuous manner from one corner of the test box. The casting process was carried out using a 45°-inclined chute between the mixer and the open spot of the Square-Box set-up. The filling height was thus fixed for all the experiments. The filling period was controlled to 18 ± 1 s, hence resulting in a casting rate of 2.5–2.8 L/s (9.1–10.2 m^3/h), or an average casting rate of 2.7 L/s (9.6 m^3/h). The continuous concrete placement enables relatively high-energy flow conditions of the FR-SCC.

The passing ability of the investigated mixtures was evaluated using the Square-Box set-up equipped with four rows of 10-mm diameter reinforcing bar grids positioned in horizontal and vertical configurations, in addition to one longitudinal rebar through the whole length of the set-up (Fig. 1). The reinforcing-bar grids were placed in the middle of each of the four close-surfaced channels. Moreover, the dynamic stability of the investigated mixtures was evaluated by carrying out this test without presence of any reinforcing bars. It is worth mentioning that the confined flow conditions encountered during repair of elongated elements (e.g., RC beams) were simulated using the selected continuous closed-surface flow (about 10-m^3/s casting rate) and restricted section width of 100 mm of the proposed Square-Box set-up. The clear spacing of the reinforcing steel bars was set to 45 mm, corresponding to three-time the nominal maximum size of aggregate, which is typically encountered in this type of application. On the other hand, the geometry of the proposed Square-Box test led to more confined and restricted flow conditions and longer flow distances compared to the T-Box, L-Box, and filling-box set-ups. Indeed, the channel width of 100 mm is 50% tighter than those of the T-Box and L-Box set-ups (200 mm) [29, 31], and filling-box test (300 mm) [34]. On the other hand, the clear spacing between the vertical rebars and the Square-Box set-up's walls is 45 mm which is lower than that of the L-Box set-up of 60 mm. The closed surface of the Square-Box set-up also led to more restricted and confined flow conditions compared to those of the conventional L-Box and T-Box set-ups. Furthermore, a comparable sample volume (48 vs. 45 L) travels longer flow distances (2.4 vs. 0.5 m) across tighter flow width (100 vs. 300 mm)

Table 3 Rheological properties of the investigated cement paste and mortar mixtures

Mortar No	Corresponding FR-SCC mixture	$\tau_{0\text{-}P}$ (Pa)	$\mu_{p\text{-}P}$ (Pa.s)	$\tau_{0\text{-}M}$ (Pa)	$\mu_{p\text{-}M}$ (Pa.s)
M3	FRC-3	0.95	0.032	13.49	3.07
M4	FRC-4	1.01	0.040	6.58	3.55
M5	FRC-5	1.09	0.040	7.05	3.54
M6	FRC-6	1.22	0.040	7.96	3.55
M7	FRC-7	1.27	0.043	4.61	3.24
M10	FRC-10	1.58	0.045	5.78	3.39

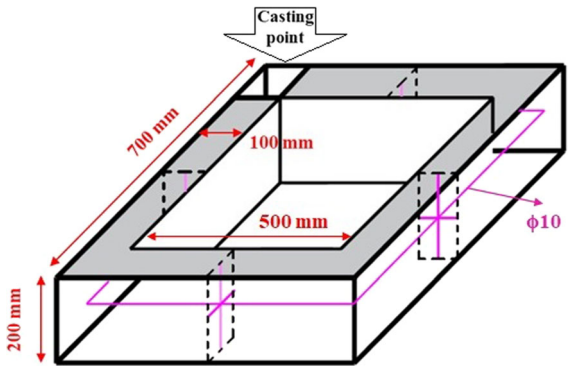

Fig. 1 Schematics of the proposed Square-Box test to evaluate the passing ability and dynamic stability of the FR-SCC mixtures

and under greater casting rate (2.7 vs. 0.7 L/s) through the Square-Box set-up compared to those experienced in the filling-box test [34]. Therefore, the Square-Box test can more realistically simulate the concrete flow conditions for highly restricted sections compared to the L-Box, T-Box, and filling-box tests.

As shown in Fig. 2a, immediately after casting, the cast beam was divided in 5 different sections (i = 1 to 5) using separators inserted just behind the reinforcing grids at middle of the channels. Then, 5 cylindrical samples measuring 100 mm in diameter and 200 mm in height were taken from each section i = 1 to 5 to evaluate the variation of concentration and distribution of coarse aggregate and steel fibers at different distances from the casting point. The extracted samples from each section were wet-sieved on 5-mm sieve and then dried. The extracted fibers and coarse aggregate were then separated using a magnet and weighted. The volumetric content of fiber-coarse aggregate samples in unit volume of concrete and the PSD of extracted coarse aggregate were determined for each sample. The fibers and coarse aggregate were remixed to determine the packing density of fiber-coarse aggregate combination using the ICT device [35–37]. The variation of ratio of the volumetric content ($\varphi_{F\text{-}i} + \varphi_{\text{CA-}i}$)-to-the packing density ($\varphi_{\text{max-F-A-}i}$) of fiber-coarse aggregate combination obtained at different distances (i = 1 to 5) from the casting point relative to the reference mixture ($\varphi_{F+\text{CA-Ref}}/\varphi_{\text{max-F+CA-Ref}}$) was calculated.

Accordingly, a heterogeneity index ($HI_{F+\text{CA-i}}$) to assess the dynamic stability and passing ability of the investigated FR-SCC mixtures was defined, as follows:

$$\text{HI}_{F+\text{CA}-i} = \frac{\frac{\varphi_{F-i}+\varphi_{\text{CA}-i}}{\varphi_{\max-F+\text{CA}-i}}}{\frac{\varphi_{F-\text{Ref}}+\varphi_{\text{CA}-\text{Ref}}}{\varphi_{\max-F+\text{CA}-\text{Ref}}}} \times 100\% \quad (3)$$

where $\varphi_{F\text{-}i}$, $\varphi_{\text{CA-}i}$, $\varphi_{F\text{-Ref}}$, and $\varphi_{\text{CA-Ref}}$ are the volumetric contents of fibers and coarse aggregate in sample i (i = 1 to 5) and reference mixture, respectively. Moreover, $\varphi_{\text{max-}F+\text{CA-}i}$ and $\varphi_{\text{max-F+}CA\text{-}Ref}$ are the packing density values of fiber-coarse aggregate combinations obtained in each section (i = 1 to 5) and reference mixture, respectively. The blocking (BI) and dynamic segregation (DSI) indices of the investigated mixtures were evaluated using the coefficient of variation ($C.O.V.$) of $HI_{F+\text{CA-}i}$ values obtained at five sections (i = 1 to 5) of the testing set-up with and without reinforcing bars, respectively, as follows:

$$\begin{aligned}\text{BI} &= \text{C.O.V.}\ (\text{HI}_{F+CA-i})_{i\,=\,1\ to\ 5} \\ &= \frac{\sigma(\text{HI}_{F+\text{CA}-i})_{i\,=\,1\ to\ 5}}{\text{Avg}(\text{HI}_{F+\text{CA}-i})_{i\,=\,1\ to\ 5}} \\ &\quad \times 100\%\text{C.O.V.}\ (\text{HI}_{F+\text{CA}-i})_{i\,=\,1\ to\ 5} \\ &= \frac{\sigma(\text{HI}_{F+\text{CA}-i})_{i\,=\,1\ to\ 5}}{\text{Avg}(\text{HI}_{F+\text{CA}-i})_{i\,=\,1\ to\ 5}} \\ &\quad \times 100\%,\ \text{in presence of reinforcing bars}\end{aligned} \quad (4)$$

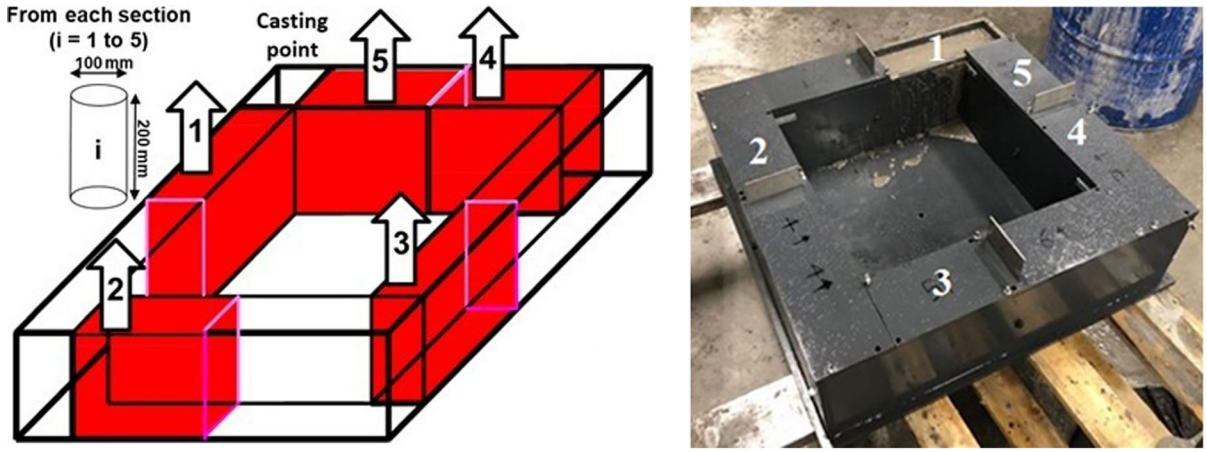

Fig. 2 (**a**) Sampling method from each section (i = 1–5) of (**b**) the proposed Square-Box test set-up

$$\mathrm{DSI} = \mathrm{C.O.V.}\ (\mathrm{HI}_{F+\mathrm{CA}-i})_{i\ =\ 1\ to\ 5} = \frac{\sigma(\mathrm{HI}_{F+\mathrm{CA}-i})_{i\ =\ 1\ to\ 5}}{Avg(\mathrm{HI}_{F+\mathrm{CA}-i})_{i\ =\ 1\ to\ 5}} \times 100\%, \quad \text{without reinforcing bars} \qquad (5)$$

where $\sigma(HI_{F+CA-i})_{i=1\ to\ 5}$ and $\mathrm{Avg}(\mathrm{HI}_{F+\mathrm{CA}-i})_{i=1\ to\ 5}$ are the standard deviation and average of HI_{F+CA-i} values obtained in sections i = 1 to 5, respectively. The obtained BI and DSI indices for the investigated FR-SCC mixtures are summarized in Table 4.

3 Results and discussion

The coupled effects of flow distance, relative-solid packing-fraction ($\varphi/\varphi_{\max}$) of fiber-coarse aggregate combination (> 5 mm), and rheological properties of the mortars on passing ability and dynamic stability of the investigated FR-SCC mixtures (BI and DSI indices—Eqs. 4 and 5) were evaluated in this section.

3.1 Effect of flow distance on heterogeneous performance of FR-SCC

The HI values (Eq. 3) obtained at different distances from the casting point in the Square-Box without and with presence of reinforcing bars are presented in Fig. 3a and b, respectively. It is worth mentioning that the distance from the casting point, illustrated in Fig. 3, correspond to the distance travelled by concrete to reach the middle of each section.

As can be observed in Fig. 3, lower HI values (< 100%) were obtained at longer flow distances. This reflects the decrease in relative-solid packing-fraction of fiber-coarse aggregate combination with the flow distance from the casting point relative to the reference mixture. This can be due to dynamic segregation and blocking of fibers and coarse aggregate across the Square-Box test. The maximum and minimum variations in the $\varphi/\varphi_{\max}$ of fiber-coarse aggregate were obtained for FRC-4 and FRC-7 mixtures, respectively. This can be attributed to the rheology of their corresponding mortar mixtures, their fiber content, and fiber-coarse aggregate characteristics, which is further discussed in the following sections. Moreover, the results presented in Fig. 3a and b revealed higher variations in HI indices in the presence of reinforcing bars (70.7% < HI-with bar < 126.4%) compared to those obtained without any obstacles (82.7% < HI-without bar < 109.7%). This can be attributed to the blockage of fibers and coarse aggregate due to presence of reinforcing bars.

3.2 Blocking

The blocking indices (BI) of the investigated FR-SCC mixtures were correlated to their relative solid packing-fraction ($\varphi/\varphi_{\max}$) of fiber-coarse aggregate combinations, as well as the yield stress ($\tau_{0\text{-}M}$) and plastic

Table 4 Workability results of the investigated FR-SCC mixtures

Mix	FRC-3	FRC-4	FRC-5	FRC-6	FRC-7	FRC-10
BI (%)	12.9	26.0	19.1	11.3	9.9	19.1
DSI (%)	7.1	11.9	2.8	3.2	1.3	4.5

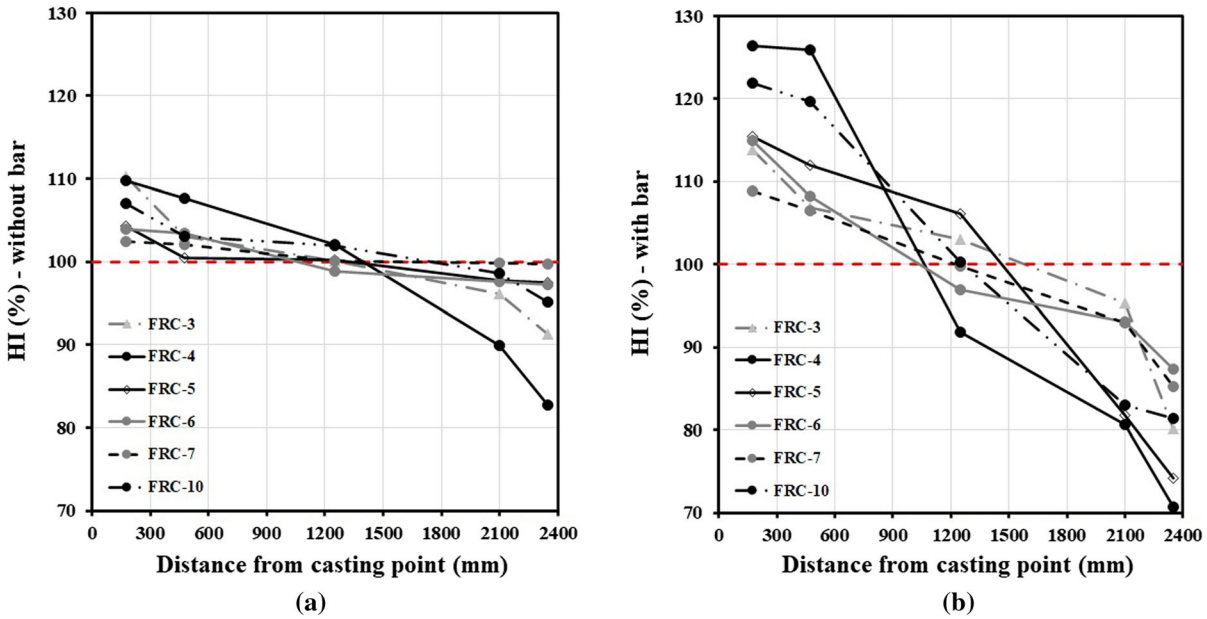

Fig. 3 Effect of flow distance on fiber-coarse aggregate distribution in the Square-Box test (**a**) without and (**b**) in presence of reinforcing bars

viscosity ($\mu_{p\text{-}M}$) values of their corresponding mortar mixtures, as follows:

$$BI\ (\%) = A_1 \times V_f^{A_2} \times \left(\frac{\varphi}{\varphi_{\max}}\right)^{A_3} \times A_4^{\tau_{0-M}} \times A_5^{\mu_{p-M}} + A_6 \quad (6)$$

where V_f is volumetric content of fibers and A_1 to A_6 are the adjustment factors reflecting the effect of different characteristics of suspended and suspending phases. A Microsoft Excel solver was then developed to obtain the adjustment factors leading to the closest BI values to the experimental ones. The results of the established correlation are shown in Eq. (7) and Fig. 4. As can be observed in Fig. 4, the blocking indices of the investigated FR-SCC mixtures are in good agreement with the fiber content, $\varphi/\varphi_{\max}$ of fiber-coarse aggregate combinations, and rheological properties of their corresponding mortar matrix (R^2 of 1.0 and RMSE of 0.111%).

$$\mathrm{BI}\ (\%) = 587.869 \times \frac{V_f^{0.630} \times \left(\frac{\varphi}{\varphi_{\max}}\right)^{11.4549}}{0.967^{\tau_{0-M}} \times 0.288^{\mu_{p-M}}} + 0.564 \quad (7)$$

According to the obtained adjustment factors in Eq. (7), increasing the fiber content and $\varphi/\varphi_{\max}$ of fiber-coarse aggregate and decreasing the yield stress and plastic viscosity of the mortar resulted in higher blockage indices. The increasing in fibers and coarse aggregate contents can result in higher interaction between the solid phase (fibers and coarse aggregate) with the reinforcing bars and confining formwork walls, hence leading to higher blockage. On the other hand, mortar mixtures with higher yield stress and plastic viscosity can exert higher drag forces on fibers

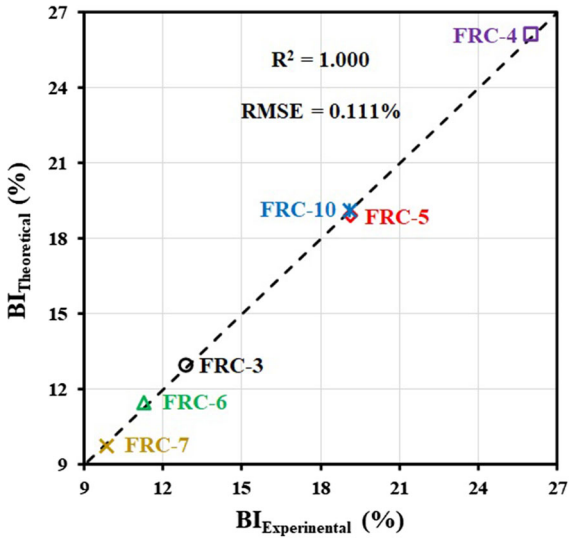

Fig. 4 Comparison between the experimental BI indices of the investigated FR-SCC mixtures and those obtained using Eq. (7)

and coarse aggregate, hence leading to lower risk of separation of the suspended and suspending phases (lower BI values). Among different parameters, φ/φ_{max} of fiber-coarse aggregate combinations showed the most significant effect on passing ability of the investigated mixtures, rather than fiber content and rheology of mortar.

Furthermore, the passing ability of FR-SCC mixtures evaluated using the proposed Square-Box test is compared to the blocking indices obtained from the L-Box set-up (UBI_{LB} in Table 3). The ultimate blocking indices in the proposed Square-Box test (UBI_{SB}) were firstly evaluated, as follows:

$$UBI_{SB}\ (\%) = \frac{\left(\frac{\varphi}{\varphi_{max}}\right)_1 - \left(\frac{\varphi}{\varphi_{max}}\right)_5}{\left(\frac{\varphi}{\varphi_{max}}\right)_{Ref}} \times 100\% \quad (8)$$

where $\left(\frac{\varphi}{\varphi_{max}}\right)_1$, $\left(\frac{\varphi}{\varphi_{max}}\right)_5$, and $\left(\frac{\varphi}{\varphi_{max}}\right)_{Ref}$ correspond to the relative-solid packing-fraction of fiber-coarse aggregate mixtures in samples taken from Sects. 1 and 5 of the proposed Square-Box set-up (Fig. 2a) and reference mixture, respectively. As can be observed in Fig. 5, the investigated mixtures exhibited significantly higher blocking in the Square-Box test (UBI_{SB} of 23.6–55.7%) compared to those obtained in the L-Box set-up (UBI_{LB} of 11.4–19.5%). This can be due to higher flow distance travelled by the concrete through the proposed Square-Box test (2.4 m) compared to the horizontal channel (0.7 m) of the L-Box set-up.

Moreover, as mentioned earlier, the concrete is subjected to more restricted and confined flow conditions in the proposed Square-Box test compared to that in the L-Box test. Indeed, the L-Box and Square-Box set-ups are equipped with 1 and 4 rows of reinforcing bars with clear spacings of 60 and 45 mm between the rebars and Square-Box walls, respectively. Furthermore, the flow in the L-Box set-up is a free-surface flow type while it was confined at 4 sides in the Square-Box test. These can lead to higher interaction between the reinforcing bars and fiber-coarse aggregate skeleton in the Square-Box test, hence leading to higher flow-induced blockage compared to the L-Box flow. This suggests that the L-Box set-up cannot sufficiently simulate the confined flow conditions of FR-SCC mixtures compared to the Square-Box test. Accordingly, low blocking indices in L-Box test may not guarantee high passing ability passing through the narrow zones such those that can be encountered in repair applications. This can highlight the proficiency of the proposed Square-Box test to simulate the flow conditions that FR-SCC experiences in repair applications.

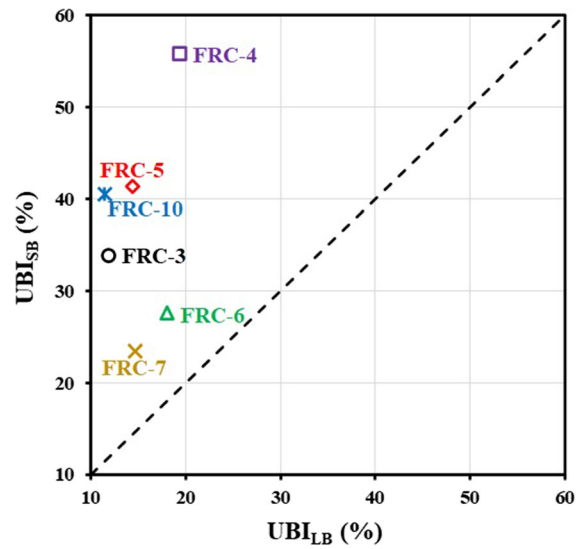

Fig. 5 Comparison between the blocking results of the investigated FR-SCC mixtures in the L-Box (UBI_{LB}) and proposed Square-Box tests (UBI_{SB})

3.3 Dynamic stability

The coupled effect of rheological properties of mortar, fiber content, and φ/φ_{max} of fiber-coarse aggregate combinations on dynamic segregation of the investigated FR-SCC mixtures was evaluated. This was carried out similarly to the BI indices, using Eq. (6) and a developed Microsoft Excel solver. The results of the established correlation are shown in Eq. (9) and Fig. 6.

$$UBI_{SB}\ (\%) = \frac{\left(\frac{\varphi}{\varphi_{max}}\right)_1 - \left(\frac{\varphi}{\varphi_{max}}\right)_5}{\left(\frac{\varphi}{\varphi_{max}}\right)_{Ref}} \times 100\% \quad (9)$$

As can be observed in Fig. 6, the established Eq. (9) can well predict the dynamic segregation of the investigated FR-SCC mixtures as a function of volumetric content of fibers (V_f), φ/φ_{max} of fiber-coarse aggregate combination, as well as yield stress ($\tau_{0\text{-}M}$) and plastic viscosity ($\mu_{p\text{-}M}$) of their corresponding mortar matrices (R^2 of 0.970 and RMSE of 0.611%). According to the obtained adjustment factors in Eq. (9), increasing yield stress and plastic viscosity of mortar led to higher dynamic stability of the investigated FR-SCC mixtures. This can be attributed to higher drag forces exerted on fibers and coarse aggregate, hence reducing the risk of separation of the solid phase (fibers and coarse aggregate) and suspending mortar.

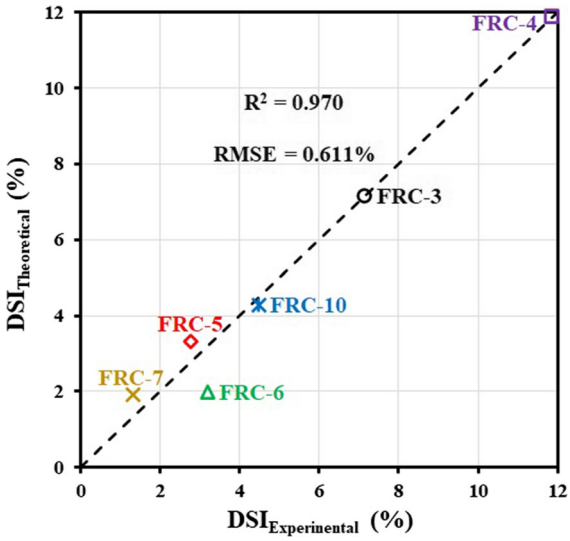

Fig. 6 Comparison between the experimental DSI indices of the investigated FR-SCC mixtures and those obtained using Eq. (9)

On the other hand, the risk of dynamic segregation of the investigated FR-SCC mixtures increased for higher fiber volume and φ/φ_{max} of fiber-coarse aggregate. This is in contradiction to the positive effect of the φ/φ_{max} of coarse aggregate on dynamic stability of plain SCC mixtures through the T-Box set-up, as reported in literature [26]. This can be due to different flow conditions through the T-Box and Square-Box tests. In fact, the flow through the proposed Square-Box test is two times more confined (100-mm width) compared to the T-Box test (200-mm wide channel). Moreover, the T-Box flow is free-surface while concrete flow in the Square-Box test is surrounded by 4 walls. Furthermore, unlike the straight flow direction in the T-Box test, the investigated FR-SCC mixtures were subjected to three 90°-turning directions at the corners of the close-circuit in Square-Box set-up. These can lead to higher risk of interlocks between the coarse aggregate and fibers, as well as higher interactions between the solid phase (fibers and coarse aggregate) and the Square-Box set-up's walls for the mixtures proportioned with higher φ/φ_{max} of fiber-coarse aggregate combinations. The Square-Box test was developed to test the flowability and passing ability under highly complex conditions that can be encountered in both pre-cast and cast-in-place applications, including repair applications involving the use of SCC and FR-SCC. In some applications, the repair material needs to flow in 90° angles necessitating changes in flow directions that can lead to higher risk of blockage. Such complex geometry can be found in casting T-Beam bridge girders and repair of columns and reinforced concrete beams and girders.

The dynamic stability of FR-SCC mixtures assessed using the Square-Box test is compared to the dynamic segregation indices obtained froam the T-Box set-up ($UDSI_{TB}$ in Table 2). The ultimate dynamic segregation index in the Square-Box set-up ($UDSI_{SB}$) was evaluated, as follows:

$$UDSI_{SB}\ (\%) = \frac{\left(\frac{\varphi}{\varphi_{max}}\right)_1 - \left(\frac{\varphi}{\varphi_{max}}\right)_5}{\left(\frac{\varphi}{\varphi_{max}}\right)_{Ref}} \times 100\% \quad (10)$$

where $\left(\frac{\varphi}{\varphi_{max}}\right)_1$, $\left(\frac{\varphi}{\varphi_{max}}\right)_5$, and $\left(\frac{\varphi}{\varphi_{max}}\right)_{Ref}$ corresponds to the relative-solid packing fraction of fiber-coarse

aggregate mixtures in samples taken from Sects. 1 and 5 of the Square-Box test (without reinforcing bars: Fig. 2b), and the reference mixture, respectively.

As can be observed in Fig. 7, the majority of the investigated mixtures showed relatively higher dynamic segregation indices in the T-Box set-up ($UDSI_{TB}$ of 12.2–49.6%) compared to those obtained in the Square-Box test ($UDSI_{SB}$ of 2.7–27.0%) for majority of the investigated mixtures. This can be related to the higher flow distance that concrete travels in the T-Box test (9.0 m) [40] than that in the Square-Box test (2.4 m). Although the T-Box set-up allowed longer flow distance, the confined flow conditions in repair application are more realistically reproduced using the proposed Square-Box test, as mentioned earlier. This may suggest that the dynamic segregation in T-Box test is overestimated compared to that can occur under confined flow conditions of the repair application.

3.4 Filling ability classification of FR-SCC mixtures

The filling ability of the investigated FR-SCC mixtures can be classified by plotting their blocking indices (BI–Eq. 6) to dynamic segregation indices (DSI–Eq. 7) presented in Table 5. As shown in Table 5, three different classes corresponding to relatively low, medium, and high dynamic stability and passing ability were defined according to the measured DSI and BI values. As shown in Fig. 8, the investigated FR-SCC mixtures were classified in three different filling ability levels, including (i) high filling ability (Green zone: low DSI and BI values), (ii) medium filling ability (Purple zone: low to medium DSI and BI values), and (iii) low filling ability (Red zone: high DSI and BI values).

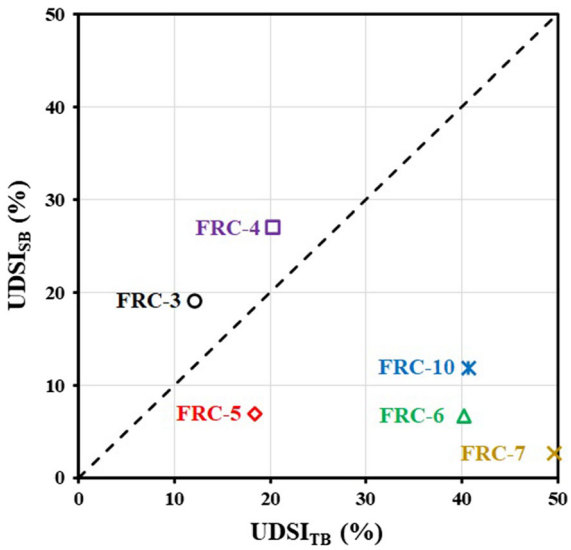

Fig. 7 Comparison between the dynamic segregation results of the investigated FR-SCC mixtures in the T-Box ($UDSI_{TB}$) and proposed Square-Box tests ($UDSI_{SB}$)

According to the established classification, the majority of the investigated mixtures exhibited medium and high filling ability levels, except the FRC-4 mixture (low filling ability). On the other hand, the FRC-6 and FRC-7 mixtures showed the highest filling ability among the investigated FR-SCC mixtures. Accordingly, the characteristics of FR-SCC mixtures with high filling ability are summarized in Table 6 based on the properties of their corresponding cement paste (volumetric content and rheology), mortar matrix (rheology), PSD of aggregate, macro-steel fiber content, and fiber-coarse aggregate (volumetric content and packing density). This is worth mentioning that the characteristics summarized in Table 6 are only preliminary recommendations established based on limited FR-SCC mixtures investigated in this study. Further studies are thus required to establish more comprehensive recommendations considering wider ranges of characteristics of coarse aggregate (PSD and PD), volume and type of fibers, W/B ratio, and paste volume.

3.5 Impact of flow-induced heterogeneity on mechanical performance of FR-SCC

As shown in the previous sections, the FR-SCC mixtures exhibited heterogeneous distribution of fibers and aggregate due to dynamic segregation and blocking in the Square-Box test. This was reflected by the variations of volumetric content and packing density of the fiber-coarse aggregate compared to the reference mixture. Inadequate homogeneities can impact mechanical performance of FR-SCC. Unfavorable mechanical performance of FR-SCC can lead to lower bond with the substrate concrete [18]. The effect of flow-induced heterogeneity on dissimilar mechanical properties of the investigated mixtures determined at different distances from the casting point was evaluated.

In addition to the samples taken for dynamic segregation measurements, two cylindrical samples,

Table 5 Recommended dynamic stability and passing ability criteria to establish the filling ability classification of FR-SCC

Flow performance level	Low	Medium	High
Dynamic stability	DSI > 8%	4% ≤ DSI ≤ 8%	DSI < 4%
Passing ability	BI > 21%	15% ≤ BI ≤ 21%	BI < 15%
Filling ability	Low filling ability	Medium filling ability	High filling ability

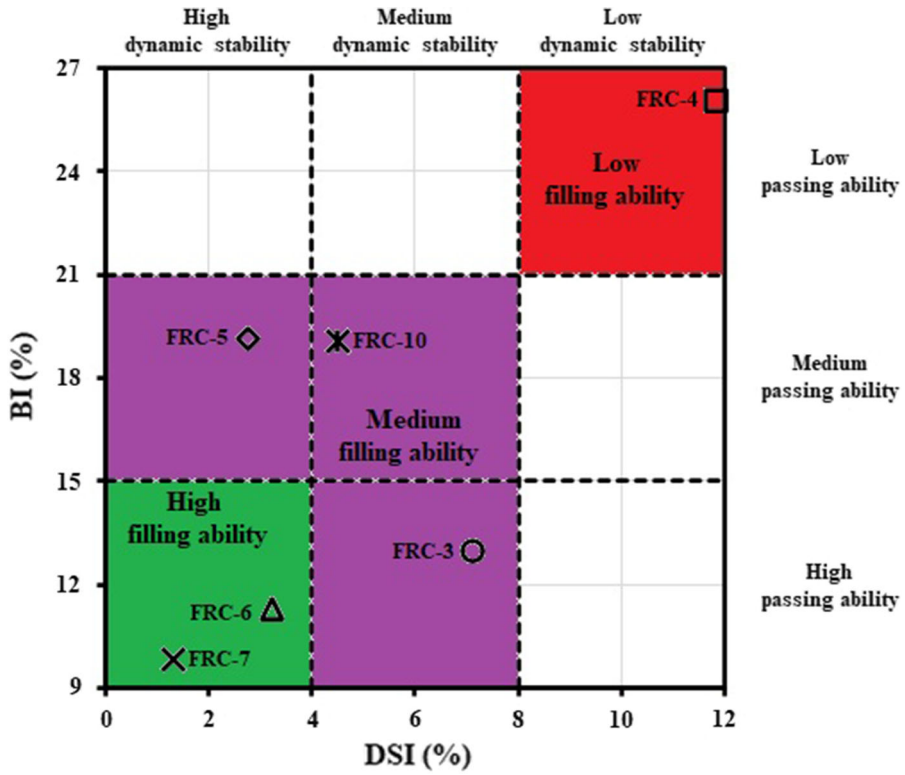

Fig. 8 Filling ability-based classifications of the investigated FR-SCC mixtures: passing ability (BI) versus dynamic stability (DSI) indices

measuring 100 mm in diameter and 200 mm in height, were taken from each section (i = 1 to 5) of the Square-Box set-up with no reinforcing bars to determine compressive strength. It is worthy to mention that these samples could not be taken for the configuration with presence of reinforcing bars. Indeed, enough quantity of concrete was not available to be sampled for compressive strength measurements after sampling for blocking measurements. It was due to blockage occurred in first three sections of the reinforced Square-Box set-up. The compressive strength ($f'_{c\text{-}i}$) of the taken samples corresponding to each section (i = 1 to 5) was measured after 28 days of curing at 100% relative humidity condition. The flow-induced dissimilarity in compressive strength values across the cast element was evaluated using a compressive-strength heterogeneity index (CSHI). The CSHI is defined as the coefficient of variation (C.O.V.) of the ratio of $f'_{c\text{-}i}$ values obtained in sections i = 1 to 5-to-the compressive strength of the investigated reference mixtures before any segregation ($f'_{c\text{-Ref}}$ values in Table 3), as follows:

Table 6 Preliminary recommendation of characteristics of FR-SCC mixtures that can exhibit high filling ability

Mixture constituents	Properties	Recommended ranges
Cement paste	Paste volume: V_P (%)	30–33
	Yield stress: $\tau_{0\text{-}P}$ (Pa)	1.22–1.27
	Plastic viscosity: $\mu_{p\text{-}P}$ (Pa.s)	0.040–0.043
Mortar	Yield stress: $\tau_{0\text{-}M}$ (Pa)	4.61–7.96
	Plastic viscosity: $\mu_{p\text{-}M}$ (Pa.s)	3.24–3.55
Aggregate	Volumetric sand-to-total aggregate ratio: S/A	0.55
	Particle-size distribution of coarse aggregate	PSD-1 and PSD-3
Macro steel fiber	Fiber volume: V_f (%)	0.12–0.25
Fiber-coarse aggregate combination	Packing density: $\varphi_{\max}$	0.536–0.554
	Relative-solid packing-fraction: $\varphi/\varphi_{\max}$	0.521–0.528

$$\text{CSHI}\ (\%) = \text{C.O.V.}\left(\frac{f'_{c-i}}{f'_{c-\text{Ref}}}\right)_{i\,=\,1\ to\ 5} = \frac{\sigma\left(\frac{f'_{c-i}}{f'_{c-\text{Ref}}}\right)_{i\,=\,1\ to\ 5}}{Avg\left(\frac{f'_{c-i}}{f'_{c-\text{Ref}}}\right)_{i\,=\,1\ to\ 5}} \times 100\%, \quad \text{without reinforcing bars} \tag{11}$$

where $\sigma\left(\frac{f'_{c-i}}{f'_{c-\text{Ref}}}\right)$ and $\text{Avg}\left(\frac{f'_{c-i}}{f'_{c-\text{Ref}}}\right)_{i\,=\,1\ to\ 5}$ are the standard deviation and average of the relative compressive strength of the samples at each section (i = 1 to 5) to that of the reference mixture, respectively. As can be observed in Fig. 9, the CSHI values determined using Eq. (11) are in good agreement with dynamic segregation indices of the investigated mixtures in the Square-Box test, obtained using Eq. (5) (DSI in Table 4). According to the established correlation, higher dynamic segregation can lead to more dissimilar compressive strength values at different sections of the cast element. Therefore, it can be concluded that an appropriate and uniform mechanical performance across the repaired element can be achieved by ensuring homogeneous flow performance of the used FR-SCC.

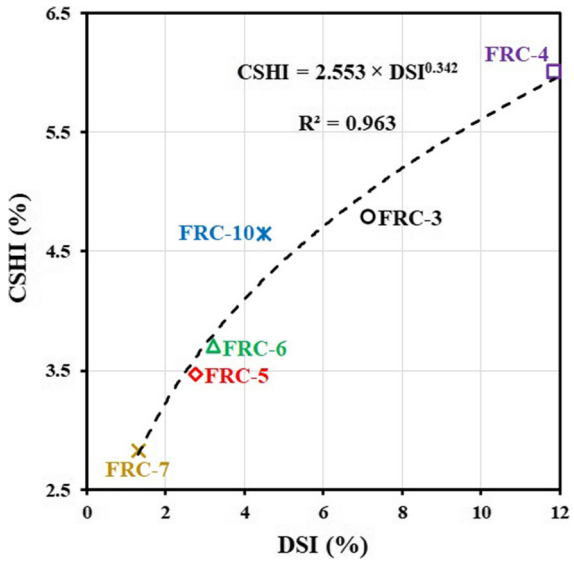

Fig. 9 Relationship between the CSHI and DSI indices of the investigated FR-SCC mixtures

4 Conclusions

In this study, workability of various FR-SCC mixtures for repair applications was investigated as biphasic suspension of steel fibers and coarse aggregate (> 5 mm) in a suspending mortar, containing cement paste and aggregate finer than 5 mm. The mixtures exhibiting high passing ability and medium to high dynamic stability in the conventional L-Box and T-Box set-ups were identified. However, these conventional tests cannot properly simulate the confined and restricted flow conditions. Accordingly, a new empirical Square-Box test was proposed to evaluate the passing ability and dynamic stability of the selected FR-SCC mixtures under confined flow conditions in presence and without reinforcing bars, respectively. The proposed Square-Box test consisted of a close-surface and close-circuit of four rectangular

channels, hence providing more confined and restricted flow conditions compared to the T-Box and L-Box set-ups. Based on the obtained experimental results, the following concluding remarks can be drawn:

- Unlike the conventional L-Box and T-Box tests, the proposed Square-Box test could successfully simulate the flow conditions during casting of FR-SCC mixtures, including the flow distance and confinement, wall effect, and presence of highly congested reinforcing bars.
- The dynamic segregation and blocking indices resulting from the Square-Box are well correlated to the coupled effect of fiber volume, relative-solid packing-fraction (φ/φ_{max}) of fiber-coarse aggregate combination, and rheological properties of mortar matrix. It is important to note that these correlations were developed using FR-SCC mixtures covering a wide range of paste volumes (V_P of 27–33%), fiber contents (V_f of 0.12–0.50%), coarse aggregate particle-size distributions (PSD1-3), relative-solid packing fractions of fiber-coarse aggregate combinations (φ/φ_{max} of 0.521–0.552), and high-range water-reducer dosages (HRWR of 1036 to 2600 ml/100 kg of binder). These mixtures were prepared with single hooked-end steel fiber measuring 30 mm in length (aspect ratio of 55) and a fixed water-to-binder ratio of 0.42, and exhibited a targeted slump flow of 680 ± 20 mm.
- The volumetric content and φ/φ_{max} of fibers and coarse aggregate showed negative effect on both dynamic stability and passing ability of FR-SCC mixtures. On the other hand, increasing yield stress and plastic viscosity of the suspending mortar mixtures enhanced the homogeneous performance of the investigated FR-SCC mixtures. The flow-induced heterogeneities of the investigated FR-SCC mixtures were found more controlled by characteristics of fibers and coarse aggregate rather than the rheology of mortar.
- The investigated FR-SCC mixtures exhibited significantly higher blocking indices through the proposed Square-Box test (UBI_{SB} values of 24–56%) compared to those obtained using the L-Box test (UBI_{LB} values of 11–20%). On the other hand, the dynamic segregation indices obtained using the T-Box set-up ($UDSI_{TB}$ values of 12–50%) were found overestimated ($UDSI_{SB}$ values of 3–27% in the proposed Square-Box test). Furthermore, the fiber volume and φ/φ_{max} of fiber-coarse aggregate showed opposite effects on dynamic segregation indices determined using the T-Box and Square-Box tests, due to their different flow conditions.
- A new filling ability classification was established for FR-SCC mixtures. The specifications of the FR-SCC mixtures with high dynamic stability and passing ability properties were recommended. These include the appropriate ranges of volumetric content and rheology of cement paste, viscoplastic properties of mortar, PSD of aggregate, macro-steel fiber content, and φ/φ_{max} of fiber-coarse aggregate combination for confined and restricted flow conditions (e.g., repair application).
- The heterogeneous flow performance of the investigated FR-SCC mixtures was found in good agreement with heterogeneous mechanical performance obtained at different flow distances. According to the established correlation, higher dynamic segregation led to higher dissimilar compressive strength values across the repaired/-cast element.

Acknowledgements The authors wish to thank the financial support of the National Science and Engineering Research Council of Canada (NSERC) and the eight industrial partners participating in the NSERC Industrial Research Chair (IRC) on Development of Flowable Concrete with Adapted Rheology and Their Application in Concrete Infrastructures, held by Professor Ammar Yahia at the Université de Sherbrooke.

Authors' contribution NN: Conceptualization, Methodology, Software, Validation, Formal analysis, Investigation, Data curation, and Writing–Original draft. MH: Conceptualization, Methodology, Software, Validation, Formal analysis, Investigation, Resources, Data curation, Writing–Review original and edited drafts, and Supervision. AY: Conceptualization, Methodology, Formal analysis, Investigation. Resources, Writing–Review original and edited Drafts, Supervision, and Project administration, KHK: Conceptualization, Methodology, Formal analysis, Investigation, Writing–Review original and edited drafts, Supervision, and Project administration.

Declarations

Conflict of interest The authors declare that they have no known competing financial interests or personal relationships that could have appeared to influence the work reported in this paper.

References

1. Wang J, Dai Q, Si R, Ma Y, Guo S (2020) Fresh and mechanical performance and freeze-thaw durability of steel fiber-reinforced rubber self-compacting concrete (SRSCC). J Clean Prod 277:123180. https://doi.org/10.1016/j.jclepro.2020.123180
2. Cattaneo S, Giussani F, Mola F (2012) Flexural behaviour of reinforced, prestressed and composite self-consolidating concrete beams. Constr Build Mater 36:826–837. https://doi.org/10.1016/j.conbuildmat.2012.06.001
3. Khayat KH, Kassimi F, Ghoddousi P (2014) Mixture design and testing of fiber-reinforced self-consolidating concrete. ACI Mater J 111(2):143–152. https://doi.org/10.14359/51686722
4. Ferrara L, Bamonte P, Caverzan A, Musa A, Sanal I (2012) A comprehensive methodology to test the performance of Steel Fibre Reinforced Self-Compacting Concrete (SFR-SCC). Constr Build Mater 37:406–424. https://doi.org/10.1016/j.conbuildmat.2012.07.057
5. Dhonde HB, Mo YL, Hsu TTC, Vogel J (2007) Fresh and hardened properties of self-consolidating fiber-reinforced concrete. ACI Mater J 104(5):491–500. https://doi.org/10.14359/18905
6. ASTM C1399/C1399M-10 (2015) Standard test method for obtaining average residual-strength of fiber-reinforced concrete, West Conshohocken, PA; ASTM International. https://dx.doi.org/https://doi.org/10.1520/C1399_C1399M-10R15
7. ASTM C1609/C1609M-19a (2020) Standard test method for flexural performance of fibre-reinforced concrete (Using Beam With Third Point Loading), West Conshohocken, PA; ASTM International. https://dx.doi.org/https://doi.org/10.1520/C1609_C1609M-19A
8. Song Q, Yu R, Shui Z, Wang X, Rao S, Lin Z (2018) Optimization of fibre orientation and distribution for a sustainable ultra-high performance fibre reinforced concrete (UHPFRC): experiments and mechanism analysis. Constr Build Mater 169:8–19. https://doi.org/10.1016/j.conbuildmat.2018.02.130
9. Zhang L, Zhao J, Fan C, Wang Z (2020) Effect of surface shape and content of steel fiber on mechanical properties of concrete. Adv Civ Eng 2020:8834507. https://doi.org/10.1155/2020/8834507
10. Sorelli LG, Meda A, Plizzari GA (2006) Steel fiber concrete slabs on ground: A structural matter. ACI Struct J 103(4):551–558. https://doi.org/10.14359/16431
11. Di Prisco M, Mauri M, Scola M (2006) A new design for stabilizing ground slopes, In: Proceedings of the 2nd fib congress, Napoli, Italy, ID 4-1 on CD-ROM. http://hdl.handle.net/11311/536592
12. El-Dieb AS, Reda Taha MM (2012) Flow characteristics and acceptance criteria of fiber-reinforced self-compacted concrete (FR-SCC). Constr Build Mater 27(1):585–596. https://doi.org/10.1016/j.conbuildmat.2011.07.004
13. Žirgulis G, Švec O, Geiker MR, Cwirzen A, Kanstad T (2016) Influence of reinforcing bar layout on fibre orientation and distribution in slabs cast from fibre-reinforced self-compacting concrete (FRSCC). Struct Concr 17(2):245–256. https://doi.org/10.1002/suco.201500064
14. Boulekbache B, Hamrat M, Chemrouk M, Amziane S (2010) Flowability of fibre-reinforced concrete and its effect on the mechanical properties of the material. Constr Build Mater 24(9):1664–1671. https://doi.org/10.1016/j.conbuildmat.2010.02.025
15. Jasiūnienė E, Cicėnas V, Grigaliūnas P, Rudžionis Ž, Navickas AA (2018) Influence of the rheological properties on the steel fibre distribution and orientation in self-compacting concrete. Mater Struct 51:103. https://doi.org/10.1617/s11527-018-1231-y
16. Yoo DY, Zi G, Kang ST, Yoon YS (2015) Biaxial flexural behavior of ultra-high-performance fiber-reinforced concrete with different fiber lengths and placement methods. Cem Concr Compos 63:51–66. https://doi.org/10.1016/j.cemconcomp.2015.07.011
17. Hwang S-D, Khayat KH (2008) Effect of mixture composition on restrained shrinkage cracking of self-consolidating concrete used in repair. ACI Mater J 105(5):498–508. https://doi.org/10.14359/19980
18. Kassimi F, El-Sayed AK, Khayat KH (2014) Performance of fiber-reinforced self-consolidating concrete for repair of reinforced concrete beams. ACI Struct J 111(6):1277–1286. https://doi.org/10.14359/51687031
19. Safdar M, Matsumoto T, Kakuma K (2016) Flexural behavior of reinforced concrete beams repaired with ultra-high performance fiber reinforced concrete (UHPFRC). Compos Struct 157:448–460. https://doi.org/10.1016/j.compstruct.2016.09.010
20. Issa CA, Assaad JJ (2017) Stability and bond properties of polymer-modified self-consolidating concrete for repair applications. Mater Struct 50(1):28. https://doi.org/10.1617/s11527-016-0921-6
21. Diab AM, Abd Elmoaty AEM, Tag Eldin MR (2017) Slant shear bond strength between self compacting concrete and old concrete. Constr Build Mater 130:73–82. https://doi.org/10.1016/j.conbuildmat.2016.11.023
22. Arezoumandi M, Wirkman C, Volz JS (2018) Performance of fiber-reinforced self-consolidating concrete for repair of bridge substructures. Structure 15:320–328. https://doi.org/10.1016/j.istruc.2018.07.015
23. Kassimi F, El-Sayed AK, Khayat KH (2021) Flexural behavior of fiber-reinforced SCC for monolithic and composite beams. J Adv Concr Technol 19(8):937–949. https://doi.org/10.3151/jact.19.937
24. Abed MA, Fořt J, Naoulo A, Essa A (2021) Influence of polypropylene and steel fibers on the performance and crack repair of self-compacting concrete. Materials 14(19):5506. https://doi.org/10.3390/ma14195506
25. Voigt T, Bui VK, Shah SP (2004) Drying shrinkage of concrete reinforced with fibers and welded-wire fabric. ACI Mater J 101(3):233–241. https://doi.org/10.14359/13119
26. Koura BIO, Hosseinpoor M, Yahia A (2020) Coupled effect of fine mortar and granular skeleton characteristics on dynamic stability of self-consolidating concrete as a diphasic material. Constr Build Mater 263:120131. https://doi.org/10.1016/j.conbuildmat.2020.120131
27. Hosseinpoor M, Koura BIO, Yahia A (2021) Rheo-morphological investigation of static and dynamic stability of self-consolidating concrete: a biphasic approach. Cem Concr Compos 121:104072. https://doi.org/10.1016/j.cemconcomp.2021.104072

28. Hosseinpoor M, Koura BIO, Yahia A (2021) New diphasic insight into the restricted flowability and granular blocking of self-consolidating concrete: effect of morphological characteristics of coarse aggregate on passing ability of SCC. Constr Build Mater 308:125001. https://doi.org/10.1016/j.conbuildmat.2021.125001
29. Esmaeilkhanian B, Feys D, Khayat KH, Yahia A (2014) New test method to evaluate dynamic stability of self-consolidating concrete. ACI Mater J 111(3):299–307. https://doi.org/10.14359/51686573
30. ASTM C1621/C1621M-17 (2017) Standard test method for passing ability of self-consolidating concrete by J-Ring. West Conshohocken, PA; ASTM International. https://doi.org/10.1520/C1621_C1621M-17
31. EFNARC, European Project Group (2005) The European guidelines for self-compacting concrete: specification, production and use
32. ASTM C1611/C1611M-18 (2018) Standard Test method for slump flow of self-consolidating concrete. West Conshohocken, PA; ASTM International. https://doi.org/10.1520/C1611_C1611M-18
33. Kuroiwa S, Matsuoka Y, Hayakawa M, Shindoh T (1993) Application of super workable concrete to construction of a 20-story building. ACI Symposium Publication vol 140, p 147–162
34. Khayat KH (1999) Workability, testing, and performance of self-consolidating concrete. ACI Mater J 96(3):346–353. https://doi.org/10.14359/632
35. Nordtest (1994) Method (NT BUILD 427) for Fresh Concrete: Compactibility with IC-tester (Intensive Compaction Tester) Proj. 1005-91, Nord. Scand. Inst. 1-4, ISSN 0283-7153. www.nordtest.org
36. Aïssoun BM (2011) Étude de l'influence des caractéristiques des granulats sur la performance des bétons fluides à rhéologie adaptée (in French). M.Sc. Thesis, Université de Sherbrooke. http://savoirs.usherbrooke.ca/handle/11143/1590
37. Nouri N, Hosseinpoor M, Yahia A, Khayat KH (2022) Coupled effect of fiber and granular skeleton characteristics on packing density of fiber-aggregate mixtures. Constr Build Mater 342:127932. https://doi.org/10.1016/j.conbuildmat.2022.127932
38. Hosseinpoor M, Koura BIO, Yahia A, Kadri EH (2021) Diphasic investigation of the visco-elastoplastic characteristics of highly flowable fine mortars. Constr Build Mater 270:121425. https://doi.org/10.1016/j.conbuildmat.2020.121425
39. Hosseinpoor M, Koura BIO, Yahia A (2021) Rheo-morphological investigation of Reynolds dilatancy and its effect on pumpability of self-consolidating concrete. Cem Concr Compos 117:103912. https://doi.org/10.1016/j.cemconcomp.2020.103912
40. Esmaeilkhanian B, Khayat KH, Yahia A, Feys D (2014) Effects of mix design parameters and rheological properties on dynamic stability of self-consolidating concrete. Cem Concr Compos 54:21–28. https://doi.org/10.1016/j.cemconcomp.2014.03.001

Publisher's Note Springer Nature remains neutral with regard to jurisdictional claims in published maps and institutional affiliations.

Springer Nature or its licensor holds exclusive rights to this article under a publishing agreement with the author(s) or other rightsholder(s); author self-archiving of the accepted manuscript version of this article is solely governed by the terms of such publishing agreement and applicable law.